Journal of Pharmacological Sciences 136 (2018) 97–106

Contents lists available at ScienceDirect

Journal of Pharmacological Sciences

journal homepage: www.elsevier.com/locate/jphs

Full paper

Effects of Histidine-rich glycoprotein on erythrocyte aggregation and hemolysis: Implications for a role under septic conditions

Hui Zhong [a], Hidenori Wake [a], Keyue Liu [a], Yuan Gao [a], Kiyoshi Teshigawara [a], Masakiyo Sakaguchi [b], Shuji Mori [c], Masahiro Nishibori [a, *]

[a] Department of Pharmacology, Okayama University Graduate School of Medicine, Dentistry and Pharmaceutical Sciences, 2-5-1 Shikata-cho, Kita-ku, Okayama 700-8558, Japan
[b] Department of Cell Biology, Okayama University Graduate School of Medicine, Dentistry and Pharmaceutical Sciences, 2-5-1 Shikata-cho, Kita-ku, Okayama 700-8558, Japan
[c] School of Pharmacy, Shujitsu University, 1-6-1 Nishikawahara, Naka-ku, Okayama 703-8516, Japan

ARTICLE INFO

Article history:
Received 16 August 2017
Received in revised form
19 October 2017
Accepted 9 November 2017
Available online 24 November 2017

Keywords:
Eryptosis
Aggregation
Hemolysis
Sepsis
Histidine-rich glycoprotein (HRG)

ABSTRACT

The apoptotic process of erythrocytes is known as eryptosis, and is characterized by phosphatidylserine (PS) expression on the outer membrane. PS-positive erythrocytes are increased in sepsis, and PS is believed to facilitate coagulation of erythrocytes and activate macrophages. However, the relationship between eryptosis and abnormal coagulation in sepsis is still not fully understood.

Histidine-rich glycoprotein (HRG) inhibits immunothrombus formation by regulating neutrophils and vascular endothelial cells. In the present study, we subjected isolated erythrocytes to Zn^{2+} stimulation, which activated their aggregation and PS expression. We then determined the Zn^{2+} contents in septic lung and kidney tissues, and found that they were elevated, suggesting that eryptosis was enhanced in these tissues. Erythrocyte adhesion to endothelial cells was also significantly increased after Zn^{2+} stimulation, and this effect was inhibited by HRG. Finally, we examined HRG treatment in septic model mice, and found that HRG decreased hemolysis, possibly due to its ability to bind heme.

Our study demonstrated a novel Zn^{2+}-initiated aggregation/thrombus formation pathway. We also showed the regulatory role of HRG in this pathway, together with the ability of HRG to inhibit hemolysis under septic conditions. HRG supplementation might be a novel therapeutic strategy for inflammatory disorders, especially sepsis.

1. Introduction

Eryptosis is the apoptotic-like suicidal process of erythrocytes, and is characterized by cell shrinkage and phosphatidylserine (PS) expression on the outer membrane.[1] Increased eryptosis has been observed in sickle cell disease (SCD), diabetes mellitus, malaria, and beta-thalassemia.[2–5] It is believed that PS on the outer membrane of erythrocytes provides the docking spots for proteins involved in the hemostatic process.[6,7] Moreover, a significant increase in erythrocyte adhesion to endothelial cells has been observed in SCD and diabetic mellitus.[8,9] These findings suggest an active role of erythrocytes in the pathological processes of these diseases. In 2007, Kempe[10] et al. reported that erythrocytes showed an apoptotic tendency in septic patients. However, it is still not clear whether this apoptotic tendency of erythrocytes affects the development of sepsis, including the immunothrombosis during sepsis.

Immunothrombosis has been suggested to play a crucial role in sepsis and acute respiratory distress syndrome (ARDS).[11,12] However, no clinical therapy for severe immunothrombosis has yet been established. Immunothrombosis initiated by a neutrophil response to pathogen-associated molecular patterns (PAMPs) or damage-associated molecular patterns (DAMPs). This process helps to suppress the tissue invasion and dissemination of pathogens and to reduce their survival rate.[13–15] However, if the neutrophil response is overwhelmed by severe inflammation, this could lead to disseminated intravascular coagulation (DIC), and

* Corresponding author. Fax: +81 86 235 7140.
E-mail address: mbori@md.okayama-u.ac.jp (M. Nishibori).
Peer review under responsibility of Japanese Pharmacological Society.

https://doi.org/10.1016/j.jphs.2017.11.003

finally multiple organ failure.[16] Although neutrophils, platelets and vascular endothelial cells are the main effector cells involved in immunothrombosis, abnormal aggregation of erythrocytes under septic conditions may also contribute to immunothrombosis in sepsis.

Histidine-rich glycoprotein (HRG) is a 75-kDa single-chain protein produced mainly in the liver.[17] The normal plasma levels of HRG are 60–100 μg/mL (0.8–1.3 μM).[18] The primary structure of HRG contains a large number of repeated GHHPH structures, yet the protein is negatively charged under physiological pH.[19,20] Various biological functions of HRG have been reported, including the clearance of immune complex/necrotic cells and regulation of cell adhesion, angiogenesis, coagulation and fibrinolysis.[19] Many of these functions depend on the ability of HRG to form a complex with biological molecules including Zn^{2+} and heme; Zn^{2+} was reported to induce erythrocyte aggregation and eryptosis, while heme was reported to induce hemolysis.[21–25] In the previous study, we demonstrated that HRG conferred protection against lethality to septic mice by suppressing immunothrombosis and relevant inflammation.[11] However, it is still not clear whether HRG suppresses immunothrombosis through regulation of erythrocyte. In the present study, we examined the effects of HRG on the erythrocyte aggregation and PS expression induced by Zn^{2+}, which can be released by platelets. We also investigated the effects of HRG on hemin-induced hemolysis to better understand the mechanism by which HRG inhibits immunothrombosis and the anti-septic effects of HRG.

2. Materials and methods

2.1. Erythrocyte aggregation experiment

Fresh blood samples were collected from healthy volunteers, and after centrifugation at 400 × *g* for 5 min, the plasma and buffy coat were discarded. The remaining red cells were supplemented with Hank's balanced salt solution (HBSS) (Sigma Aldrich, St. Louis, MO) and centrifuged an additional 2 times. After washing, the erythrocyte suspension was adjusted to 4×10^6 cell/mL. Zn^{2+} ($ZnSO_4$, 20 μM) (Sigma Aldrich) was then added to the erythrocyte suspension to induce aggregation, along with either Histidine-rich glycoprotein (HRG) purified from human plasma,[26] Annexin V (Sigma Aldrich) or amiloride (Sigma Aldrich). Then the cell suspension was incubated at 37 °C with rotation for 1 h, and aliquoted into a 96-well plate. Aggregation of erythrocytes was observed 30 min later using an IN Cell Analyzer 2000 system (GE Healthcare, Little Chalfont, UK). Clusters of more than 10 cells were considered to be an aggregation.

2.2. Fluorescence-assisted cell sorting (FACS) analysis

The washed erythrocyte suspension was prepared as described above. The suspension was added with Zn^{2+} (20 μM) to induce PS expression. Human serum albumin (HSA), HRG or phosphate buffered saline (PBS) was added together with Zn^{2+}. After 1 h of incubation at 37 °C, cells were labeled by FITC-conjugated Annexin V (MBL, Nagoya, Japan), fixed with 4% of paraformaldehyde and quantified by fluorescence-assisted cell sorting (FACS) analysis. Intracellular Ca^{2+} levels were determined using Fluo-4 AM (Life Technologies, Carlsbad, CA) with living cells. Fluo-4 AM-loaded erythrocytes were treated with Zn^{2+} in the presence of HSA, HRG or PBS for 1 h at 37 °C. The ratio of the change in fluorescence intensity at 1 h to the initial fluorescence intensity (ΔF/F) was used as an index of intracellular Ca^{2+} increase.

2.3. Attachment of erythrocytes to vascular endothelial cells

Cells from the human endothelial hybrid cell line EA.hy926 (CRL-2922; ATCC, Manassas, VA) were used to examine the attachment of erythrocytes to vascular endothelial cells. Before the experiments, the cells were pre-cultured in a 96-well plate for 18 h, then washed twice with HBSS to remove the medium. A Zn^{2+} (20 μM)-stimulated erythrocyte suspension was added to the wells. After 30 min of incubation at 37 °C, the medium was removed and the cells were washed twice with HBSS. Cy5-conjugated monoclonal anti-CD235a antibody (Abcam, Cambridge, UK) was added to label the erythrocytes. Observation and counting of erythrocytes attached to endothelial cells was performed using an IN Cell Analyzer 2000 system.

2.4. Cecal ligation puncture (CLP) mouse model

All animal experiments were approved by the Institutional Animal Care and Use Committee of Okayama University, and performed in accordance with the guidelines of Okayama University on animal experiments. Adult male C57BL/6N mice at 8 weeks of age were obtained from SLC Japan. To induce the sepsis model, mice were anesthetized and a ligature was set below the ileocecal valve. The cecum was gently exteriorized from the peritoneal cavity and punctured twice with an 18-gauge needle, then returned to the abdomen. HRG, HSA or PBS as a control was administered through a tail vein immediately after operation. Each mouse was given 20 mg/kg in a volume of 200 μL.

2.5. Determination of mouse tissue Zn^{2+} levels and hemolysis

The Zn^{2+} levels in the tissues of septic mice were determined using a Metallo Assay Zn^{2+} LS kit (Metallogenics, Chiba, Japan). CLP model mice were sacrificed 24 h after operation. Tissues were collected and weighed, then put into tubes and supplemented with RIPA buffer (Sigma Aldrich) (4 μL/mg tissue). After crushing, the tissue homogenates were centrifuged and the resultant supernatants were used to determine the Zn^{2+} levels following the instructions included in the assay kit. Blood was drawn from the hearts of the mice and centrifuged at 800 × *g* for 5 min, and then the supernatant was collected and centrifuged again at 2000 × *g* for 5 min. Plasma was collected and the hemoglobin level was determined by the Western blot method using an anti-hemoglobin antibody (Abcam).

2.6. Determination of hemin-induced hemolysis

The level of hemin-induced hemolysis in human erythrocytes was determined by measuring the optical density (OD) at 578 nm. In brief, erythrocytes were washed and prepared as described above, and then HRG or an HRG-derived peptide (HHPHGHHPHG) was added, followed by 20 mM hemin (Sigma Aldrich). After incubation for 2.5 h at 37 °C, the cell suspension was centrifuged at 400 × *g* for 5 min. The cell pellet was collected, 1 mL of H_2O was added, and OD was used to estimate the level of hemolysis.

2.7. Determination of binding between HRG and hemin

Binding between HRG and hemin was determined by calorimetry with a Microcal iTC200 calorimeter (GE Healthcare). In brief, 1 mM of hemin was added to 0.025 mM HRG, and then the binding parameters were calculated by the software automatically.

2.8. Statistical analysis

Statistical comparisons were performed using Student *t*-test or one-way ANOVA followed by the *post hoc* Fisher's test. The mean values of data are shown along with the standard deviation (SD). *P* values less than 0.05 were considered statistically significant.

3. Results

3.1. HRG prevents Zn^{2+}-induced erythrocyte aggregation

Stimulation with 20 μM Zn^{2+} resulted in aggregation of washed human erythrocytes 1 h after incubation. Clusters of more than 10 cells were considered to be an aggregation. Aggregations formed in the Zn^{2+}-stimulated group (a typical aggregation is shown by the red arrows in Fig. 1A), while the culture containing equal levels of Mg^{2+} and Ca^{2+} did not yield any aggregations (Fig. 1A). TPEN (20 μM), a chelator for Zn^{2+}, Fe^{2+} and Mn^{2+}, abolished the effects of Zn^{2+} (Fig. 1A). HRG strongly inhibited the aggregation at a concentration of 1 μg/mL, whereas the same concentration of HSA showed no effect (Fig. 1B). HRG and HSA both strongly inhibited aggregation when the concentration was increased to 100 μg/mL (Supplementary Fig. 1). To determine the role of Ca^{2+} in the Zn^{2+}-induced aggregation, we stimulated erythrocytes under a Ca^{2+}-free condition by using Ca^{2+}-free HBSS (Fig. 1C), or by adding the Ca^{2+} channel blocker amiloride (Fig. 1D) or nimodipine (Supplementary Fig. 2). The results clearly showed that Zn^{2+} could not induce any aggregation under the Ca^{2+}-free condition. To determine the role of PS in the Zn^{2+}-induced aggregation of erythrocytes, we used Annexin V to block PS expression on the erythrocyte membrane. Annexin V (100 nM) completely inhibited the Zn^{2+}-induced aggregation (Fig. 1E).

3.2. HRG prevents Zn^{2+}-induced expression of PS on erythrocytes

The Zn^{2+} (20 μM)-induced expression of PS on erythrocytes, which was inhibited by TPEN, was not observed by other divalent cations, including Mg^{2+} and Ca^{2+} (Fig. 2A). HRG inhibited PS expression at 1 μg/mL (Fig. 2B), but HSA at the same concentration did not show any effect. HRG and HSA both inhibited PS expression when their concentrations were increased to 10 and 100 μg/mL (Fig. 2B). As shown in Fig. 2C, HRG at a low concentration (1 μg/mL) significantly inhibited the Ca^{2+} elevation in erythrocytes induced by Zn^{2+}, while HSA at the same concentration did not. HSA and HRG showed similar inhibitory effects on the intracellular Ca^{2+} elevation at higher concentrations. To test the influence of Zn^{2+} on Ca^{2+} detection, we stimulated erythrocytes with Zn^{2+} in the absence of extracellular Ca^{2+}. The results showed that the influence of Zn^{2+} on Ca^{2+} detection was minimal compared with the Zn^{2+}-induced Ca^{2+} elevation (Supplementary Fig. 3).

3.3. HRG decreased erythrocyte aggregation and PS expression on Zn^{2+}-pretreated erythrocytes

To further investigate the regulatory effects of HRG on the aggregation and PS expression of erythrocytes, we added HRG to a Zn^{2+} (20 μM)-pretreated (1 h) erythrocyte suspension that had a high population of PS-positive cells and showed significant aggregation. Surprisingly, HRG at high concentration (100 μg/mL) significantly decreased PS expression on erythrocytes. This effect of HRG was stronger than that of HSA (100 μg/mL) or TPEN (20 μM) (Fig. 3A). At lower concentration (1 μg/mL), HRG still had an inhibitory effect, while the PS expression of the HSA-treated group was not significantly different from that of the Zn^{2+}-stimulated group. Erythrocyte aggregation was also reversed by HRG at 1 μg/mL, while HSA at this concentration did not show any effect (Fig. 3B). At higher concentrations, HRG still showed stronger aggregation-reversing ability than HSA (Supplementary Fig. 4).

3.4. Zn^{2+}-induced erythrocyte adhesion to endothelial cells was inhibited by HRG

In addition to aggregation and PS expression, we also observed the level of erythrocyte attachment to vascular endothelial cells induced by stimulating erythrocytes with Zn^{2+} (20 μM) (Fig. 4A). We found that a considerable number of erythrocytes were attached to the EA.hy926 cells after Zn^{2+}-stimulation (Fig. 4A). HRG treatment significantly inhibited the attachment of erythrocytes to the vascular endothelial cell monolayer in a concentration-dependent manner (Fig. 4A and B), while HSA did not affect the adhesion. TPEN also inhibited erythrocyte adhesion, but the effect at 20 μM was weaker compared to that in the HRG (100 μg/mL)-treatment group. To examine whether vascular endothelial cells were affected by Zn^{2+}, we pretreated endothelial cells with 20 μM Zn^{2+}. However, pretreatment with Zn^{2+} did not change the adhesion of normal erythrocytes or that of Zn^{2+}-stimulated erythrocytes (Fig. 4C).

3.5. HRG treatment reduced eryptosis and hemolysis in CLP model mice

We also detected the hemolysis, PS expression and Ca^{2+} levels of mouse erythrocytes 24 h after CLP operation. Hemolysis in CLP septic mice was determined by Western blotting of plasma free hemoglobin. As shown in Fig. 5A, the level of plasma free hemoglobin was much higher in septic mice treated with PBS or HSA compared with normal mice, and the levels from HRG-treated mice were almost the same as the levels in the normal mice (Fig. 5A). Although a significant difference in PS expression was not observed among the CLP groups treated with PBS, HSA or HRG, incubation of erythrocytes for 4 h enabled the observation of beneficial effects of HRG on PS expression on erythrocytes (Fig. 5B). The intracellular Ca^{2+} levels were significantly increased in CLP mice (Fig. 5C). HRG treatment inhibited the increase in intracellular Ca^{2+} levels in erythrocytes (Fig. 5C). Finally, to clarify the Zn^{2+} dynamic in CLP mice, we determined the Zn^{2+} contents in the kidney, lung and spleen tissue. The Zn^{2+} contents in the lung and kidney homogenate were increased significantly compared to those in intact mice (Fig. 5D).

3.6. HRG treatment reduced hemin-induced hemolysis

Hemin-induced hemolysis was also inhibited by HRG and HRG-derived peptide (amino acid sequence in the Histidine-rich domain of HRG: HHPHGHHPHG) (Fig. 6A and B). Thus we further determined the binding affinity between HRG and hemin. The calorimeter experiment showed that HRG binds hemin at ratio of 1:36, and the Kd value was estimated to be 9.17×10^{-6} M (Fig. 6C) as the overall value.

4. Discussion

Pathological immunothrombosis leads to thrombotic disorder, disseminated intravascular coagulation (DIC) and facilitated sepsis development.[14–16] The cascade of immunothrombosis includes platelet activation and secretion, which may result in a local increase in Zn^{2+} concentration because of the presence of Zn^{2+} in platelet dense granules. Thus focusing on Zn^{2+}-stimulated erythrocytes might be an important new approach that could ultimately reveal the mechanism of immunothrombus formation in sepsis.

In the present study, we used 20 μM Zn^{2+} to induce PS expression and aggregation of erythrocytes. HRG significantly inhibited Zn^{2+}-induced PS expression and aggregation. We determined that intracellular Ca^{2+} elevation and membrane PS expression were necessary for Zn^{2+}-induced erythrocyte aggregation. The fact that Annexin V blocked the aggregation of erythrocytes induced by Zn^{2+} indicates that there is a causal relationship between PS expression and erythrocyte aggregation. However, PS expression appears not to be sufficient to inducing erythrocyte aggregation judging from the lack of aggregation in erythrocytes treated with platelet activating factor irrespective of the presence of PS expression (Supplementary Fig. 5A and B). We observed inhibitory effects of HRG on Zn^{2+}-induced Ca^{2+} increase even at 1 μg/mL (13 nM) (Fig. 2C). This concentration might be insufficient for 20 μM Zn^{2+} chelation. In addition, we observed that Zn^{2+} induced the adhesion of erythrocytes to endothelial cells, and this

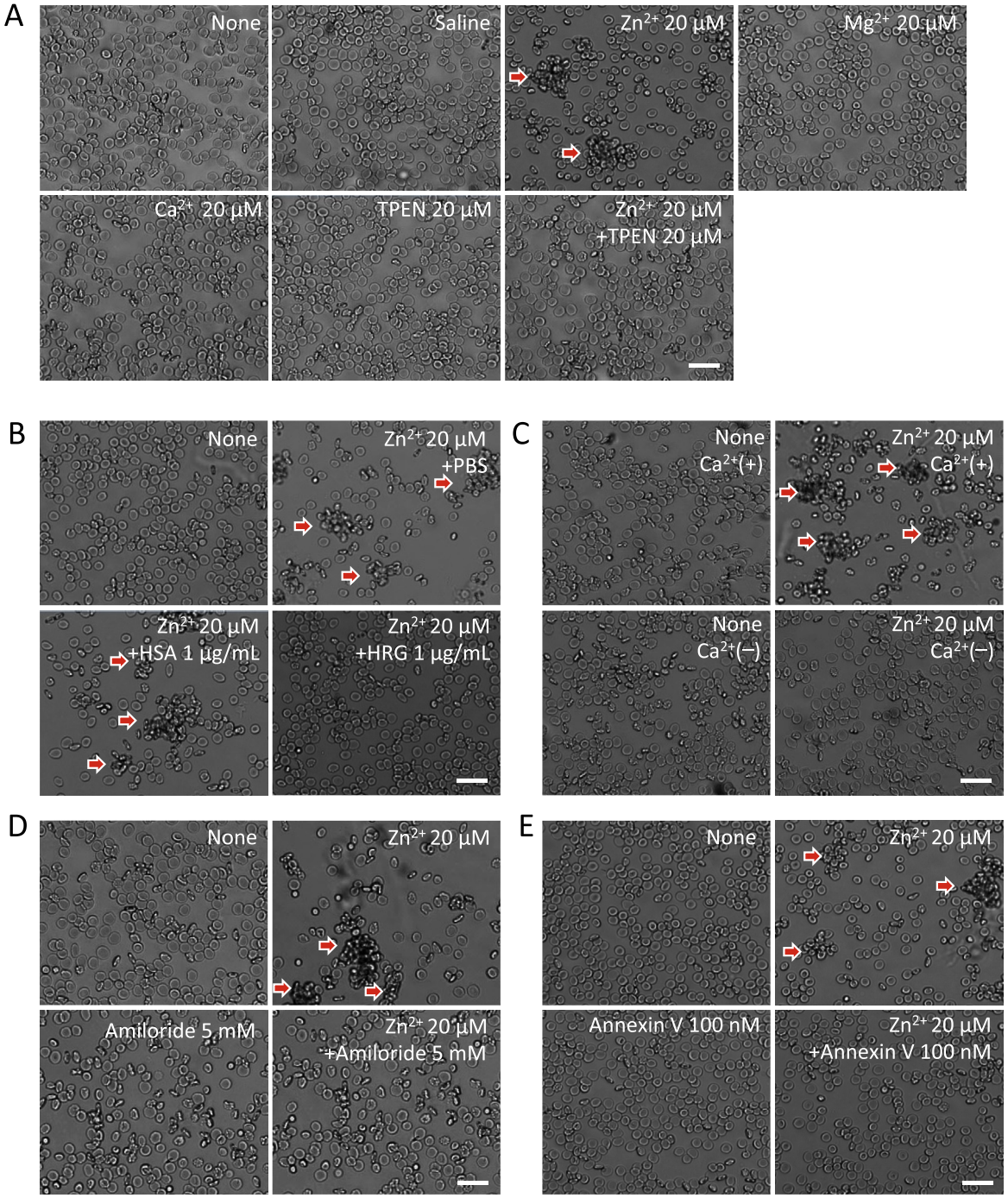

Fig. 1. Effect of HRG on Zn^{2+}-induced erythrocyte aggregation. (A) Washed erythrocytes were suspended in HBSS and stimulated by 20 μM of Zn^{2+}, Mg^{2+}, Ca^{2+} or TPEN for 1 h at 37 °C. The red arrowheads (from A to E) indicate aggregated erythrocytes. Clusters of more than 10 cells were considered to be aggregations. (B) Washed erythrocytes were suspended in HBSS and stimulated by 20 μM Zn^{2+} in the presence of 1 μg/mL of HSA, HRG or PBS for 1 h at 37 °C. Effects of higher concentrations of HRG and HSA are shown in Supplementary Fig. 1A. (C) Washed erythrocytes were suspended in HBSS or Ca^{2+}-free HBSS. Then the cell suspension was stimulated by 20 μM Zn^{2+} for 1 h at 37 °C. (D) Washed erythrocytes were suspended in HBSS, and the cell suspension was stimulated by 20 μM Zn^{2+} with or without 5 mM amiloride for 1 h at 37 °C. (E) Washed erythrocytes were suspended in HBSS and stimulated by 20 μM Zn^{2+} with or without 100 nM Annexin V for 1 h at 37 °C. Scale bars are 20 μm.

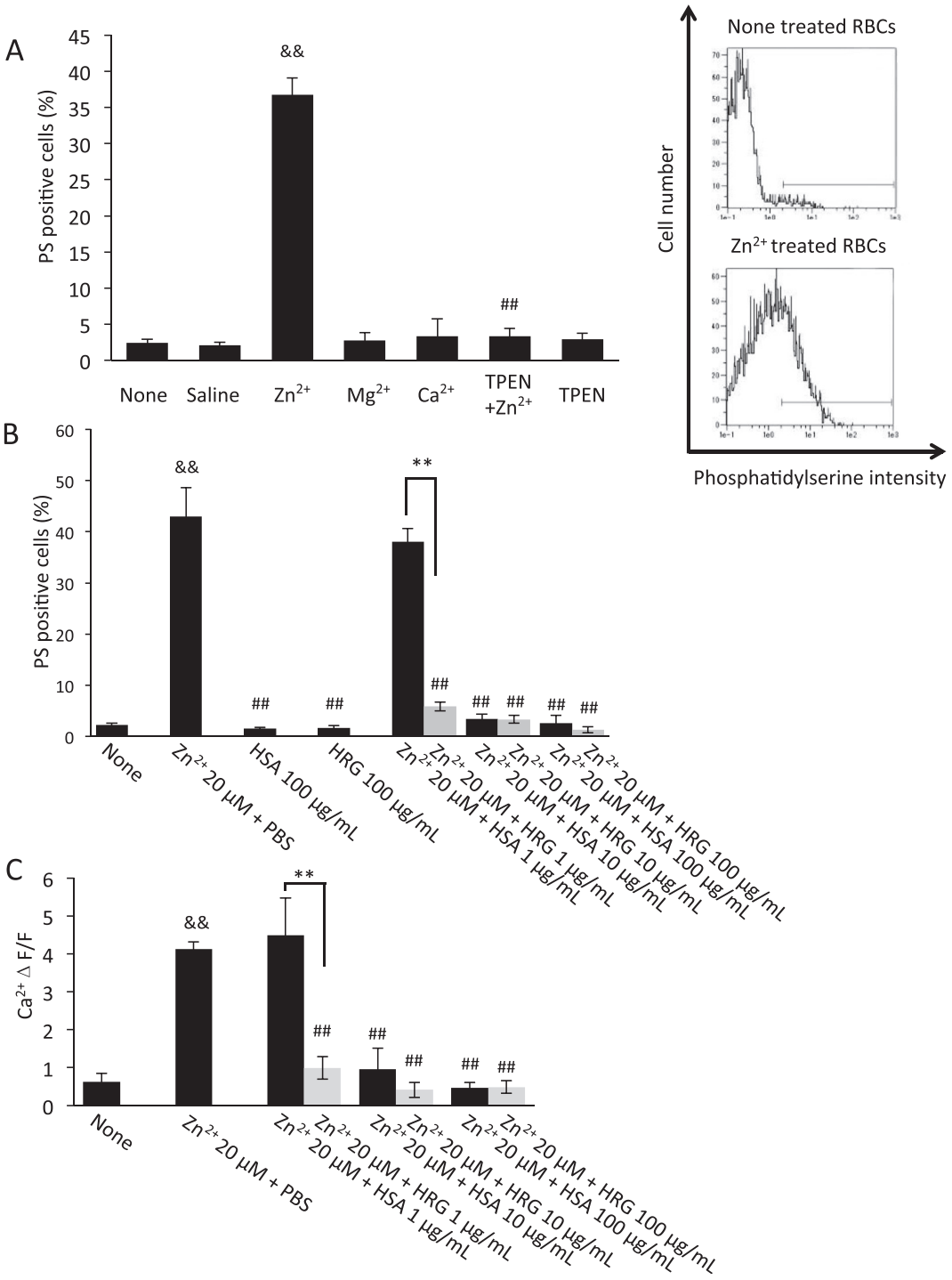

Fig. 2. Effect of HRG on Zn^{2+}-induced PS expression on erythrocytes. (A) Washed erythrocytes were suspended in HBSS and stimulated by 20 μM Zn^{2+}, Mg^{2+} or Ca^{2+}, in the presence or absence of 20 μM TPEN for 1 h at 37 °C. After incubation, PS was labeled by FITC-conjugated Annexin V. For quantification of PS-positive cells (show in the right panel; the region in the bar was considered PS-positive), FACS analysis was used. The results shown are the means ± SD of three independent experiments. $^{\&\&}P < 0.01$ vs. the saline group, $^{\#\#}P < 0.01$ vs. the Zn^{2+} group by one-way ANOVA followed by the *post hoc* Fisher's test. (B) Washed erythrocytes were suspended in HBSS and stimulated by 20 μM Zn^{2+} in the presence or absence of different concentrations of HSA or HRG for 1 h at 37 °C. The results shown are the means ± SD of three independent experiments. $^{\&\&}P < 0.01$ vs. the untreated group, $^{**}P < 0.01$ vs. the Zn^{2+} + HSA group, $^{\#\#}P < 0.01$ vs. the Zn^{2+} + PBS group by one-way ANOVA followed by the *post hoc* Fisher's test. (C) Fluo-4 AM-loaded erythrocytes were suspended in HBSS buffer. The suspension was then treated with Zn^{2+} with or without the presence of HSA, HRG or PBS for 1 h at 37 °C. The ratios of elevation of fluorescence intensity at 1 h against the initial intensity (ΔF/F) were determined. The results shown are the means ± SD of three independent experiments. $^{\&\&}P < 0.01$ vs. the untreated group, $^{**}P < 0.01$ vs. the Zn^{2+} + HSA group, $^{\#\#}P < 0.01$ vs. the Zn^{2+} + PBS group by one-way ANOVA followed by the *post hoc* Fisher's test.

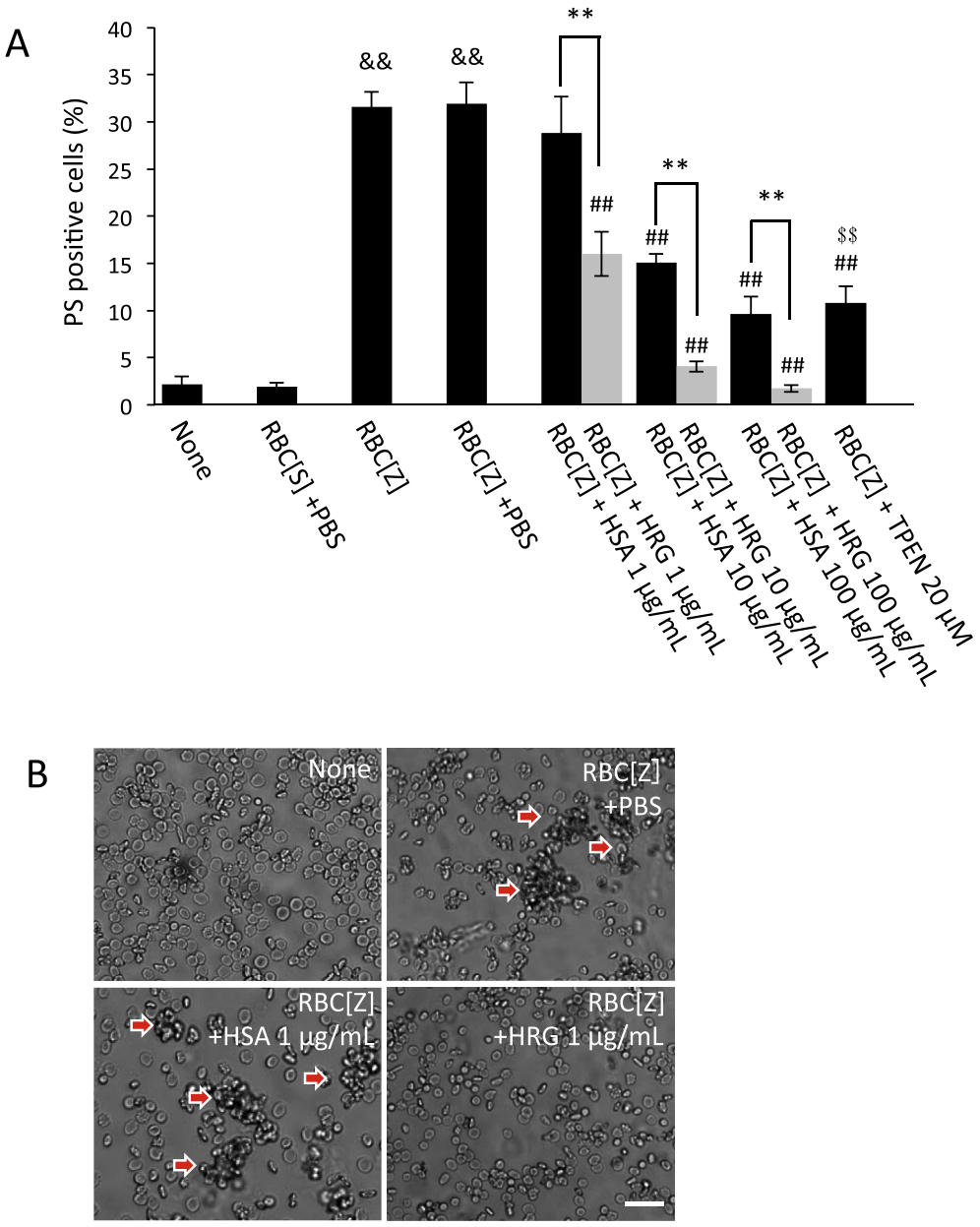

Fig. 3. Reversibility of Zn^{2+}-induced erythrocyte aggregation by HRG. (A) Washed erythrocytes were suspended in HBSS and stimulated by 20 μM Zn^{2+} (shown as RBC[Z]), or by saline (shown as RBC[S]) for 1 h at 37 °C. Then the suspension was supplemented with 1, 10, or 100 μg/mL of HSA or HRG or 20 μM of TPEN, and the incubation was continued for 30 min at 37 °C. After incubation, erythrocytes were labeled with FITC-conjugated Annexin V. PS-positive cells were quantified using FACS analysis. The results shown are the means ± SD of three independent experiments. $^{\&\&}P < 0.01$ vs. the RBC[S] + PBS group, $^{\#\#}P < 0.01$ vs. the RBC[Z] + PBS group, $^{**}P < 0.01$ vs. the RBC[Z] + HSA group, $^{\$\$}P < 0.01$ vs. the RBC[Z] + HRG 100 μg/mL group by one-way ANOVA followed by the *post hoc* Fisher's test. (B) Washed erythrocytes were suspended in HBSS and stimulated by 20 μM Zn^{2+} for 1 h at 37 °C. Then the suspension was supplemented with 1 μg/mL of HSA or HRG or with PBS as a control, and the incubation was continued for 30 min at 37 °C. Aggregation was observed using an IN Cell Analyzer 2000 system. Typical images from three independent experiments are shown. Effects of higher concentrations of HRG and HSA are shown in Supplementary Fig. 4. The scale bar represents 20 μm.

effect was not inhibited by 100 μg/mL of HSA (Fig. 4), suggesting a specific interaction between erythrocytes and HRG. However, neither a direct or indirect interaction between HRG and the Ca^{2+} channel has been reported yet. Further studies are necessary to clarify the action mechanism of HRG on erythrocytes. In any case, HRG plays a protective role with regard to Zn^{2+}-induced erythrocyte aggregation and adhesion to endothelial cells.

In a previous study, we demonstrated that plasma HRG levels decreased rapidly in septic patients as well as septic mice.[11] The decrease was due to the reduction in HRG gene expression, deposition of HRG on immunothrombi and degradation of HRG by thrombin. Decreased plasma HRG levels resulted in increased adhesion of neutrophils to vascular endothelial cells and retardation of neutrophil passage through capillary vessels. These changes were associated with an enhancement of ROS production by neutrophils.[11] Supplementary treatment of septic mice with purified HRG from human plasma remarkably suppressed immunothrombosis in the lungs as well as the associated inflammation. Thus, advanced eryptosis and erythrocyte-associated aggregation could occur in septic mice, facilitating intravascular clot formation. Consistent with these observations, in the present study we observed a marked increase in free hemoglobin in septic mice,

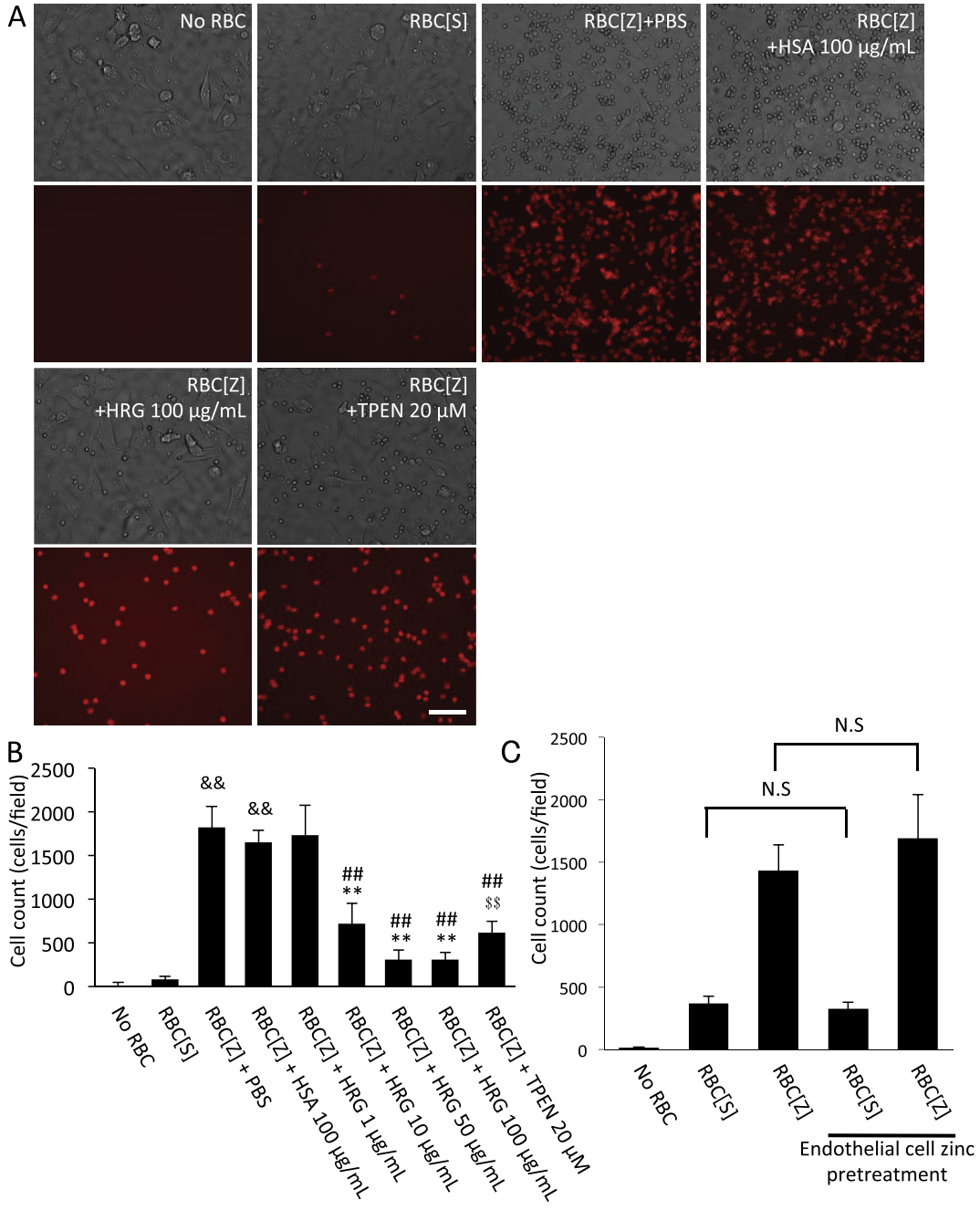

Fig. 4. Effects of HRG on Zn^{2+}-induced adhesion of erythrocytes to vascular endothelial cells. (A) Washed erythrocytes were suspended in HBSS and stimulated with 20 μM Zn^{2+} (shown as RBC[Z]) or with saline (shown as RBC[S]) for 1 h at 37 °C. Then, to the erythrocyte suspension were added PBS, HSA 100 μg/mL, HRG 100 μg/mL or TPEN 20 μM, and the mixtures were applied to an endothelial cell monolayer (EA.hy926). After 30 min of incubation, erythrocytes were labeled with anti-CD235a monoclonal antibody (observed in red immunofluorescence). Upper panels show the respective phase contrast images of the cultures. The scale bar represents 50 μm. (B) The counting of adherent erythrocytes was performed using an IN Cell Analyzer 2000 system. The results shown are the means ± SD of three independent experiments. $^{\&\&}P < 0.01$ vs. the RBC[S] group, $^{\#\#}P < 0.01$ vs. the RBC[Z] + PBS group, $^{**}P < 0.01$ vs. the RBC[Z] + HSA group, $^{\$\$}P < 0.01$ vs. the RBC[Z] + HRG 100 μg/mL group by one-way ANOVA followed by the *post hoc* Fisher's test. (C) Endothelial cells were pretreated with 20 μM Zn^{2+} for 30 min. Then saline-treated erythrocytes or 20 μM of Zn^{2+}-treated erythrocytes were added to the endothelial cells. After 30 min of incubation at 37 °C, the cells were washed, and the adherent erythrocytes were labeled with anti-CD235a monoclonal antibody and counted using an IN Cell Analyzer 2000 system. The results shown are the means ± SD of three independent experiments. N.S. = no significant difference by one-way ANOVA followed by the *post hoc* Fisher's test.

which was strongly inhibited by HRG administration (Fig. 5A). Therefore, we speculate that the aggregation-inhibiting effect of HRG observed in our in vitro experiments might prevent hemolysis and suppress clot formation under septic conditions. We showed that erythrocytes from CLP septic mice had a higher intracellular Ca^{2+} level, the incubation of erythrocytes from septic mice up-regulated the expression of PS, and both of these effects were antagonized by HRG treatment. PS expression of erythrocytes was not significantly different between the septic and normal mice when the expression levels were determined immediately after blood collection. This may have been due to efficient clearance of PS-positive erythrocytes by macrophages or the reticuloendothelial cell system in vivo, or aggregation and adhesion of PS-positive erythrocytes to vascular endothelial cells.

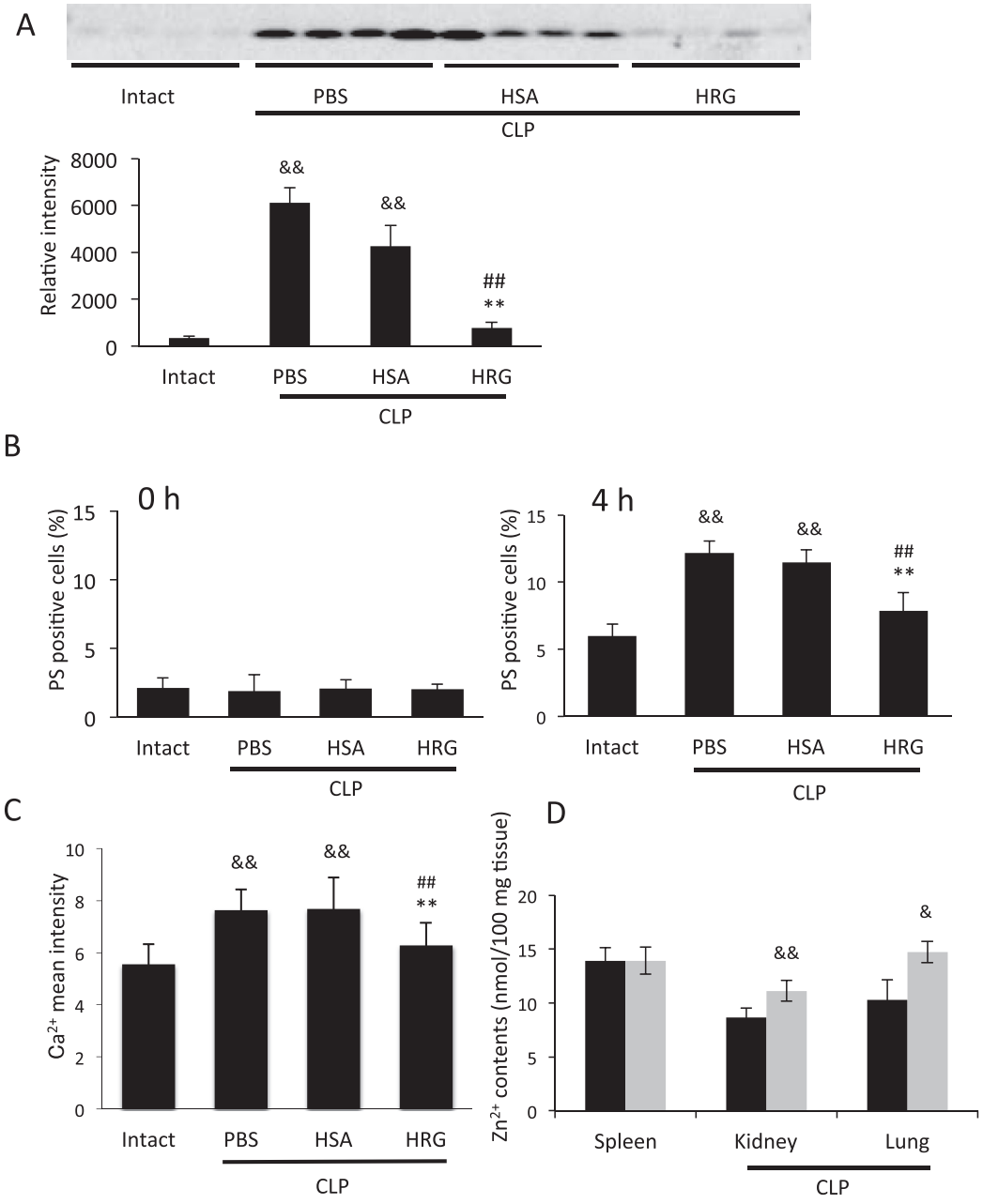

Fig. 5. Hemolysis and erythrocyte activation in CLP mice. (A) CLP septic mice treated with PBS, HSA, or HRG were sacrificed 24 h after operation. Plasma samples were electrophoresed and free hemoglobin was detected by Western blotting. The hemoglobin levels were quantified by using Image J software. The results shown are the means ± SD from 4 animals. $^{\&\&}P < 0.01$ vs. the intact group, $^{\#\#}P < 0.01$ vs. the PBS group and $^{**}P < 0.01$ vs. the HSA group by one-way ANOVA followed by the *post hoc* Fisher's test. (B) CLP mice were sacrificed 24 h after operation. Washed erythrocytes prepared immediately after collection or prepared after 4 h incubation in HBSS were labeled by FITC-conjugated Annexin V. Quantification of PS-positive cells was performed using FACS. The results are the means ± SD of 3 mice. $^{\&\&}P < 0.01$ vs. the intact group, $^{\#\#}P < 0.01$ vs. the PBS group and $^{**}P < 0.01$ vs. the HSA group by one-way ANOVA followed by the *post hoc* Fisher's test. (C) Isolated mouse erythrocytes were suspended in HBSS and intracellular Ca^{2+} was measured using Fluo 4-AM. Mean fluorescence was determined using FACS analysis. The results are the means ± SD of 7 mice for the PBS and HSA group, or 8 mice for the intact and HRG group. $^{\&\&}P < 0.01$ vs. the intact group, $^{\#\#}P < 0.01$ vs. the PBS group and $^{**}P < 0.01$ vs. the HSA group by one-way ANOVA followed by the post hoc Fisher's test. (D) Three tissues were collected from septic or normal mice. The tissue homogenates were used to determine the Zn^{2+} levels with a commercial kit. The results shown are the means ± SD of 5 animals. $^{\&}P < 0.05$, $^{\&\&}P < 0.01$ vs. the intact group by Student's *t*-test.

We also observed a higher concentration of Zn^{2+} in the lungs and kidneys, but not the spleen, of septic mice compared with normal mice. There were far fewer Gr-1-positive neutrophils in the spleen than in the lungs of CLP septic mice (data not shown), suggesting that there were fewer immunothrombi formed and a lower level of platelet secretion in the spleen than in the lungs. This may have been the reason that the Zn^{2+} levels in the spleen were not changed. Considering that Zn^{2+} was released from the aggregated platelets during thrombus formation under the septic condition, circulating erythrocytes might be exposed to high concentrations of Zn^{2+} in microvessels of the lungs and kidney. The Zn^{2+} increase and HRG decrease in plasma further contribute to excessive immunothrombus formation by inducing a dysregulation of erythrocyte aggregation and adhesion. HSA and HRG bind equal amounts of Zn^{2+} even when they are present in vastly different concentrations.[27] This indicates that both HRG and HSA could

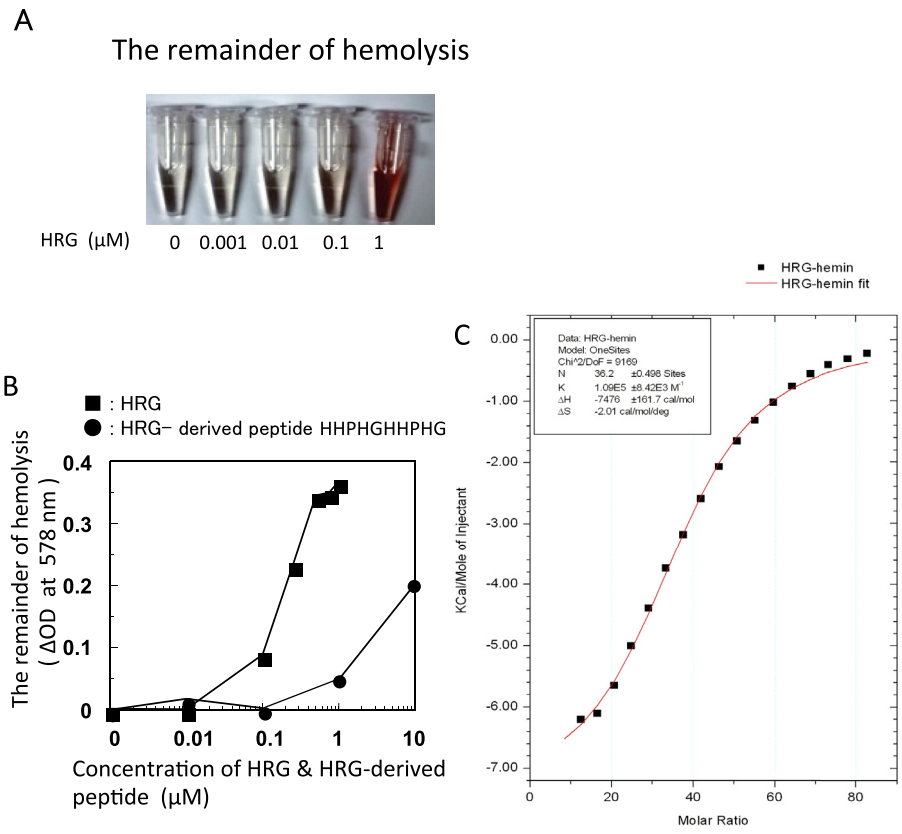

Fig. 6. Effect of HRG on hemolysis. (A) Washed human erythrocytes were diluted 100-fold with HBSS, and different concentrations of HRG were added to the suspension. Then, hemin solution (final 20 mM) was added to induce hemolysis. After 2.5 h of incubation, the cell pellet was collected and was resuspended in 1 mL of H_2O. The images are typical results from three independent experiments. (B) The results in (A) were quantified by OD measurement at 578 nm to estimate the hemolysis. (C) 1 mM of hemin was added to 0.025 mM HRG according to the instructions included with the Microcal iTC200 calorimeter. The fitting curve is shown as a red line. The Kd value was estimated to be 9.17×10^{-6} M.

regulate aggregation through chelation of Zn^{2+}. However, it is worth mentioning that HRG reversed the PS expression and aggregation of erythrocytes induced by Zn^{2+} in the present experiments, while HSA had a much weaker effect, suggesting that HRG might play a greater role than HSA in the physiological regulation of Zn^{2+}-facilitated erythrocyte aggregation and the downstream reactions. Taken together, these findings lead us to hypothesize that in tissues with massive coagulation condition. HRG might be one of the main regulators involved in reversing PS expression and aggregation of erythrocytes, based on its abilities to inhibit Ca^{2+} influx and the Zn^{2+} chelating effect.

Numerous studies have reported on the dysregulated adherence of erythrocytes to endothelial cells in SCD, malaria and diabetes.[5,7–9] However, all these adhesions are ascribable to chronic changes of erythrocytes over a prolonged period. The present study was the first to report on Zn^{2+} stimulation-induced erythrocyte adhesion over the short-term. We found that Zn^{2+} pretreatment of endothelial cells did not change the Zn^{2+}-induced adhesion of erythrocytes to endothelial cells. This result indicates that erythrocytes should be the main target of Zn^{2+} stimulation, rather than endothelial cells. HRG treatment significantly inhibited Zn^{2+}-induced adhesion of erythrocytes, but albumin did not produce any effects (Fig. 4). This adhesion may play a pivotal role in initiating thrombus formation after the activation of neutrophils and platelets in immunothrombosis. We conjecture that the strong inhibition of erythrocyte adhesion to vascular endothelial cells by HRG observed in the present study may contribute to the antithrombotic effects of HRG. Taken together, our data suggest that HRG may protect erythrocytes from adhesion to vascular endothelial cells in combination with maintaining of quiescence of circulating neutrophils and vascular endothelial cells, leading to the inhibition of immunothrombosis under septic conditions[11] and the protection of endothelial cells from damage.

We also revealed that HRG has a protective effect against hemin-induced hemolysis. As shown in our data, hemin-induced hemolysis was significantly decreased in the presence of HRG and an HRG-derived peptide (Fig. 6A and B). The number of binding sites on HRG hemin was estimated to be 36, and the apparent dissociation constant (9 μM) was determined as the overall value (Fig. 6 C). It is possible that high affinity binding may be present among 36 sites and that HRG inhibits hemin-induced hemolysis through this binding. It is also possible that HRG may inhibit hemin-induced hemolysis by another mechanism. Further studies are necessary along this line. Increased coagulation and hemolytic tendencies have been reported in patients with severe sepsis.[28–30] Extracellular heme shows strong proinflammatory potential and activates immune cells and the endothelium, thereby contributing to sepsis pathogenesis.[31–33] Taken together, HRG's inhibition of both hemin-induced hemolysis and aggregation/PS expression of erythrocytes suggests a protective effect of HRG against hemolysis under septic conditions.

In the present study, we have shown that erythrocytes play an important role in the immunothrombosis cascade through aggregation and adhesion. HRG showed protective effects in Zn^{2+}-induced aggregation and hemolysis in CLP model mice. The effects of HRG in targeting erythrocytes might be an additional mechanism involved in the anti-septic effects of HRG.

Conflict of interest disclosures

No potential conflict of interest relevant to this article was reported.

Acknowledgements

This work was supported by a Grant-in-Aid for Scientific Research (B) (No. 15H04686) from the Secom Science and Technology Foundation to M.N, a Grant-in-Aid for Young Scientists (B) (No. 17K15580) to H.W, and a Grant-in-Aid for Scientific Research (C) (No. 16K08232) to K.T. Human fresh frozen plasma was kindly provided by the Japanese Red Cross Society.

Appendix A. Supplementary data

Supplementary data related to this article can be found at https://doi.org/10.1016/j.jphs.2017.11.003.

References

1. Lang K, Lang P, Bauer C, et al. Mechanisms of suicidal erythrocyte death. *Cell Physiol Biochem*. 2005;15(5):195–202.
2. Wood BL, Gibson DF, Tait JF. Increased erythrocyte phosphatidylserine exposure in sickle cell disease: flow-cytometric measurement and clinical associations. *Blood*. 1996;88(5):1873–1880.
3. Calderon-Salinas JV, Munoz-Reyes EG, Guerrero-Romero JF, et al. Eryptosis and oxidative damage in type 2 diabetic mellitus patients with chronic kidney disease. *Mol Cell Biochem*. 2011;357(1–2):171–179.
4. Brand V, Sandu C, Duranton C, et al. Dependence of Plasmodium falciparum *in vitro* growth on the cation permeability of the human host erythrocyte. *Cell Physiol Biochem*. 2003;13(6):347–356.
5. Lang K, Roll B, Myssina S, et al. Enhanced erythrocyte apoptosis in sickle cell anemia, thalassemia and glucose-6-phosphate dehydrogenase deficiency. *Cell Physiol Biochem*. 2002;12(5–6):365–372.
6. Zwaal RFA, Schroit AJ. Pathophysiologic implications of membrane phospholipid asymmetry in blood cells. *Blood*. 1997;89(4):1121–1132.
7. Franck PF, Bevers EM, Lubin BH, et al. Uncoupling of the membrane skeleton from the lipid bilayer. The cause of accelerated phospholipid flip-flop leading to an enhanced procoagulant activity of sickled cells. *J Clin Invest*. 1985;75(1):183.
8. Wautier JL, Paton RC, Wautier MP, et al. Increased adhesion of erythrocytes to endothelial cells in diabetes mellitus and its relation to vascular complications. *N Engl J Med*. 1981;305(5):237–242.
9. Setty BNY, Kulkarni S, Stuart MJ. Role of erythrocyte phosphatidylserine in sickle red cell–endothelial adhesion. *Blood*. 2002;99(5):1564–1571.
10. Kempe DS, Akel A, Lang PA, et al. Suicidal erythrocyte death in sepsis. *J Mol Med*. 2007;85(3):273–281.
11. Wake H, Mori S, Liu K, et al. Histidine-rich glycoprotein prevents septic lethality through regulation of immunothrombosis and inflammation. *EBioMedicine*. 2016;9:180–194.
12. Frantzeskaki F, Armaganidis A, Orfanos SE. Immunothrombosis in acute respiratory distress syndrome: Cross talks between inflammation and coagulation. *Respiration*. 2017;93(3):212–225.
13. Clark SR, Ma AC, Tavener SA, et al. Platelet TLR4 activates neutrophil extracellular traps to ensnare bacteria in septic blood. *Nat Med*. 2007;13(4):463–469.
14. McDonald B, Urrutia R, Yipp BG, Jenne CN, Kubes P. Intravascular neutrophil extracellular traps capture bacteria from the bloodstream during sepsis. *Cell Host Microbe*. 2012;12(3):324–333.
15. Sun H. The interaction between pathogens and the host coagulation system. *Physiology*. 2006;21(4):281–288.
16. Ito T. PAMPs and DAMPs as triggers for DIC. *J Intensive Care*. 2014;2(1):65.
17. Koide T, Foster D, Yoshitake S, Davie EW. Amino acid sequence of human histidine-rich glycoprotein derived from the nucleotide sequence of its cDNA. *Biochemistry*. 1986;25(8):2220–2225.
18. Poon IK, Patel KK, Davis DS, Parish CR, Hulett MD. Histidine-rich glycoprotein: the Swiss army knife of mammalian plasma. *Blood*. 2011;117(7):2093–2101.
19. Jones AL, Hulett MD, Parish CR. Histidine-rich glycoprotein: a novel adaptor protein in plasma that modulates the immune, vascular and coagulation systems. *Immunol Cell Biol*. 2005;83(2):106–118.
20. Borza DB, Tatum FM, Morgan WT. Domain structure and conformation of histidine-proline-rich glycoprotein. *Biochemistry*. 1996;35(6):1925–1934.
21. Katagiri M, Tsutsui K, Yamano T, Shimonishi Y, Ishibashi F. Interaction of heme with a synthetic peptide mimicking the putative heme-binding site of histidine-rich glycoprotein. *Biochem Biophys Res Commun*. 1987;149(3):1070–1076.
22. Morgan WT. Interactions of the histidine-rich glycoprotein of serum with metals. *Biochemistry*. 1981;20(5):1054–1061.
23. Schmitt TH, Frezzatti WA, Schreier S. Hemin-induced lipid membrane disorder and increased permeability: a molecular model for the mechanism of cell lysis. *Arch Biochem Biophys*. 1993;307(1):96–103.
24. Kiyoatake K, Nagadome S, Yamaguchi T. Membrane perturbations induced by the interactions of Zn2+ ions with band 3 in human erythrocytes. *Biochem Biophys Rep*. 2015;2:63–68.
25. Kiedaisch V, Akel A, Niemoeller OM, Wieder T, Lang F. Zinc-induced suicidal erythrocyte death. *Am J Clin Nutr*. 2008;87(5):1530–1534.
26. Mori S, Takahashi HK, Yamaoka K, Okamoto M, Nishibori M. High affinity binding of serum histidine-rich glycoprotein to nickel-nitrilotriacetic acid: the application to microquantification. *Life Sci*. 2003;73(1):93–102.
27. Guthans SL, Morgan WT. The interaction of zinc, nickel and cadmium with serum albumin and histidine-rich glycoprotein assessed by equilibrium dialysis and immunoadsorbent chromatography. *Arch Biochem Biophys*. 1982;218(1):320–328.
28. Meinders AJ, Dijkstra I. Massive hemolysis and erythrophagocytosis in severe sepsis. *Blood*. 2014;124(6), 841–841.
29. Egeberg O. Blood coagulation and intravascular hemolysis. *Scand J Clin Lab Invest*. 1962;14(3):217–222.
30. Mannucci PM, Lobina GF, Caocci L, Dioguardi N. Effect on blood coagulation of massive intravascular haemolysis. *Blood*. 1969;33(2):207–213.
31. Wagener FA, Eggert A, Boerman OC, et al. Heme is a potent inducer of inflammation in mice and is counteracted by heme oxygenase. *Blood*. 2001;98(6):1802–1811.
32. Balla G, Vercellotti GM, Muller-Eberhard U, Eaton J, Jacob HS. Exposure of endothelial cells to free heme potentiates damage mediated by granulocytes and toxic oxygen species. *Lab Invest*. 1991;64(5):648–655.
33. Larsen R, Gozzelino R, Jeney V, et al. A central role for free heme in the pathogenesis of severe sepsis. *Sci Transl Med*. 2010;2(51), 51ra71–51ra71.